Supporting Information

Two Ce^{3+}-Substituted Selenotungstates Regulated by N,N-dimethylethanolamine and Dimethylamine Hydrochloride

Hai-Lou Li,[†‡] Chen Lian,[†‡] Li-Juan Chen,*[†] Jun-Wei Zhao,*[†] and Guo-Yu Yang*[‡]

[†] Henan Key Laboratory of Polyoxometalate Chemistry, College of Chemistry and Chemical Engineering, Henan University, Kaifeng, Henan 475004, China

[‡] MOE Key Laboratory of Cluster Science, School of Chemistry and Chemical Engineering, Beijing Institute of Technology, Beijing 102488, China

Figure S1. (a-b) Comparison of PXRD patterns of **1** and **2** with the simulated X-ray diffraction patterns derived from single-crystal structural analyses.

Figure S2. (a) Ball-and-stick view of the trimeric $[Ce_2(H_2O)_6(DMEA)W_4O_9(\alpha\text{-}SeW_9O_{33})_3]^{12-}$ entity in **1**. (b) Ball-and-stick view of the trimeric $[Ce_2W_4O_9(H_2O)_7(\alpha\text{-}SeW_9O_{33})_3]^{12-}$ entity in **2**. W (blue balls), Ce (brilliant yellow balls), O (red balls), Se (fuchsia balls), C (black balls), N (mazarine balls).

Figure S3. IR spectra of **1**, **2** and SeO_2.

Figure S4. TG –DTA and DSC curves of **1** and **2**.

Figure S5. ESI-MS patterns of **1** at different pH values in aqueous solution.

Figure S6. ESI-MS patterns of **2** at different pH values in aqueous solution.

Figure S7. ESI-MS patterns of **1** at different time in aqueous solution of pH = 5.0.

Figure S8. ESI-MS patterns of **1** at different time in aqueous solution of pH = 6.0.

Figure S9. ESI-MS patterns of **2** at different time in aqueous solution of pH = 5.0.

Figure S10. ESI-MS patterns of **2** at different time in aqueous solution of pH = 6.0.

Figure S11. MS spectra for the products of DPS and dodecane and GC trace of the catalytic results for the DPSO2.

Figure S12. MS spectra for the products of 4-methoxyphenylmethylsulfide and dodecane and GC trace of the catalytic results for 4-methoxyphenylmethylsulfone.

Figure S13. MS spectra for the products of 4-nitrophenylmethylsulfide and dodecane and GC trace of the catalytic results for 4-nitrophenylmethylsulfone.

Figure S14. (a) IR spectra of fresh catalyst and recycled catalyst of **1**. (b) IR spectra of fresh catalyst and recycled catalyst of **2**.

Table S1. Crystallographic Data and Structure Refinements for **1** and **2**.

Table S2. Bond Valence Sum (BVS) Calculations of All the W, Se, Ce and O Atoms in **1**.

Table S3. Bond Valence Sum (BVS) Calculations of All the W, Se, Ce and O Atoms in **2**.

Materials and methods. All chemicals were commercially purchased and used without further purification. Elemental analyses were measured with a Vario EL Cube super user V4.0.0 CHNS analyzer. IR spectra were recorded from solid samples palletized with KBr on a Perkin–Elmer FT–IR spectrometer in the range 400–4000 cm^{-1}. Powder X-ray diffraction (PXRD) patterns were collected on a Bruker D8 ADVANCE instrument with Cu Kα radiation (λ = 1.54056 Å). TG analyses were performed under a N_2 atmosphere on a Mettler–Toledo TGA/SDTA 851^e instrument with a heating rate of 10 °C min^{-1} from25 to 800 °C. The GC chromatogram was obtained on a SHIMADZU GC-2014C. Electrospray ionization mass spectrometry (ESI-MS) was performed using a Triple TOF 4600-1 mass spectrometer.

X-ray Crystallography. A suitable single crystal of **1** or **2** was picked under an optical microscope and sealed to a glass tube closed at both ends. Single-crystal X-ray diffraction intensity data for **1** or **2** were collected on a Bruker APEXII CCD detector at 296(2) K with Mo Kα monochromated radiation (λ = 0.71073 Å). Direct methods were used to solve their structures and locate the heavy atoms using the SHELXTL–97 program package.[1-2] The remaining atoms were found from successive full-matrix least-squares refinements on F^2 and Fourier syntheses. Lorentz polarization and SADABS corrections were applied. All hydrogen atoms attached to carbon and nitrogen atoms were geometrically placed and refined isotropically as a riding model using the default SHELXTL parameters. No hydrogen atoms associated with water molecules were located from the difference Fourier map. All non-hydrogen atoms were refined anisotropically except for some sodium, oxygen, nitrogen and carbon atoms and water molecules. During the course of structural refinements, seven lattice water molecules for**1** andtwenty five lattice water molecules for **2** molecule were found from the Fourier maps. But, there are still solvent accessible voids in the check cif reports of crystal structures, indicating that some lattice water molecules should exist in the structures that can't be found from the weak residual electron peaks. These water molecules are highly disordered and attempts to locate and refine them were unsuccessful. Based on TG analyses and elemental analyses, four Na^+ ions and nineteen lattice water molecules were directly added to the molecular formula of **1** whereas ten Na^+ ions and thirty-eight lattice water molecules were directly added to the molecular formula of **2**. The crystallographic data and structural refinements for **1** and**2** are listed in Table S1.

1 Sheldrick, G. M. SHELXL97, Program for Crystal Structure Refinement; University of Göttingen: Göttingen, Germany, 1997.

2 Sheldrick, G. M. SHELXS97, Program for Crystal Structure Solution; University of Göttingen: Göttingen, Germany, 1997.

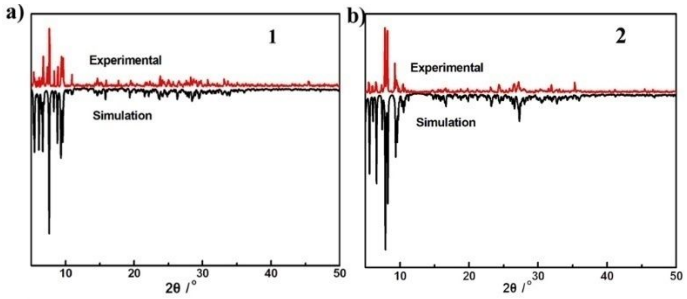

Figure S1. (a-b) Comparison of PXRD patterns of **1** and **2** with the simulated X-ray diffraction patterns derived from single-crystal structural analyses.

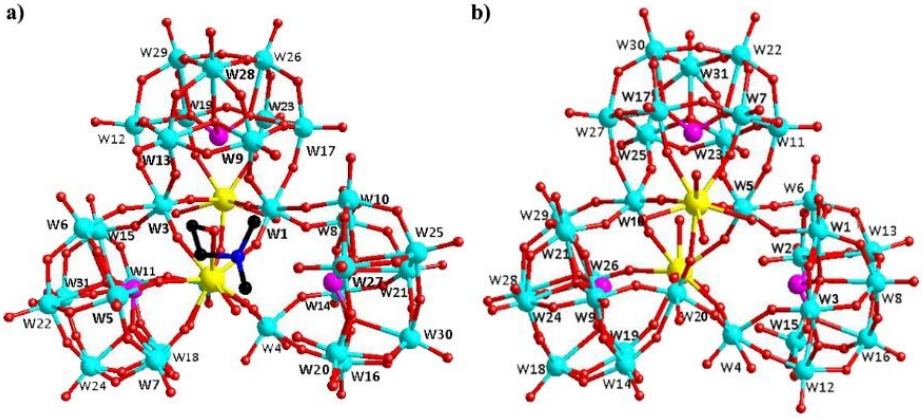

Figure S2. (a) Ball-and-stick view of the trimeric $[Ce_2(H_2O)_6(DMEA)W_4O_9(\alpha\text{-}SeW_9O_{33})_3]^{12-}$ entity in **1**. (b) Ball-and-stick view of the trimeric $[Ce_2W_4O_9(H_2O)_7(\alpha\text{-}SeW_9O_{33})_3]^{12-}$ entity in **2**. W (blue balls), Ce (brilliant yellow balls), O (red balls), Se (fuchsia balls), C (black balls), N (mazarine balls).

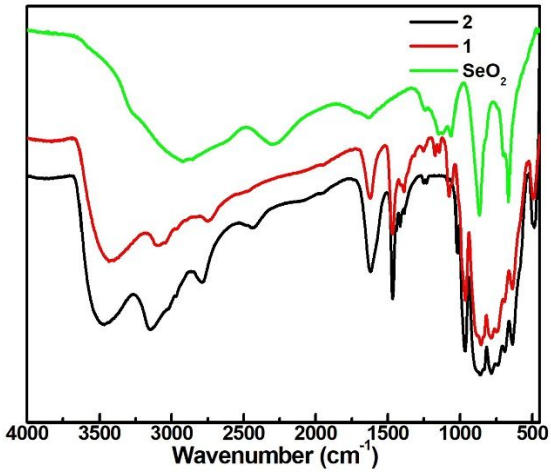

Figure S3. IR spectra of **1**,**2** and SeO_2.

IR spectra. IR spectra of **1** and **2** have been recorded between 4000–400 cm^{-1} on a Nicolet 170 SXFT–IR spectrometer by utilizing KBr pellets (Figure S3). In the low-wavenumber region, IR spectra of **1** and **2** show four characteristic vibration absorption bands attributable to $\nu(W–O_t)$, $\nu(Se–O)$, $\nu(W–O_b)$ and $\nu(W–O_c)$ are observed at 968, 892, 856 and 790 cm^{-1} for **1**, and 969, 889, 851 and 795 cm^{-1} for **2**,

respectively. Additionally, the appearance of 889-891 cm^{-1} vibration bands in the IR spectrum of SeO_2 for reference performed under the same conditions further confirms the corresponding vibration ν(Se–O) in **1** and **2**. In the high-wavenumber region, the vibration absorption band at 3402 cm^{-1} for **1**, 3415 cm^{-1} for **2** and an intense absorption band centered at 1628 cm^{-1} for **1**, 1632 cm^{-1} for **2** are respectively attributed to the stretching and bending absorption vibrations of O–H groups of water molecules. The three weak absorption bands emerging at 3128, 2772 and 1464 for **1**, 3147, 2792 and 1471 cm^{-1} for **2** are attributed to the N–H, C–H and C–N stretching vibrations, respectively, meaning the presence of organic molecules.

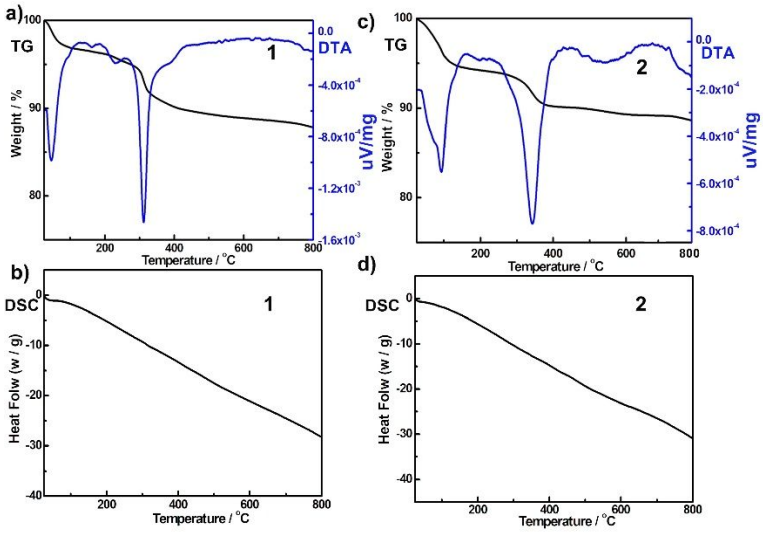

Figure S4. TG –DTA and DSC curves of **1** and **2**.

Thermogravimetric (TG) analysis. For purpose of exploring the thermal stability of **1** and **2** and ascertain their number of lattice water molecules, the TG analyses have been investigated under the flowing N_2 atmosphere from 25 to 800 °C. As exhibited in Figure S4, **1** and **2** both display the two-step weight loss process. The first step occuring between 25 and 250 °C with the weight loss of 5.10% (calcd. 5.21%) for **1** and 6.25% (calcd. 6.31%) for **2** are approximately assinged to the release of twenty-six lattice water molecules of **1** and sixty-three lattice water molecules of **2** respectively. The second weight loss of 6.03% (calcd. 5.99%) for **1** and 4.54% (calcd. 4.61%) for **2** appears in the range of 250 to 600 °C, owing to the loss of six coordination water molecules, eight protons, two DMEA groups and four dimethylamine groups of **1**, the removal of fourteen coordination water molecules, fourteen protons and ten dimethylamine groups of **2**. The total weight loss is 11.20% (calcd.11.13%) for **1** and 10.79% (calcd. 10.92%) for **2**. Clearly, the experimental values agree well with the theoretical values.

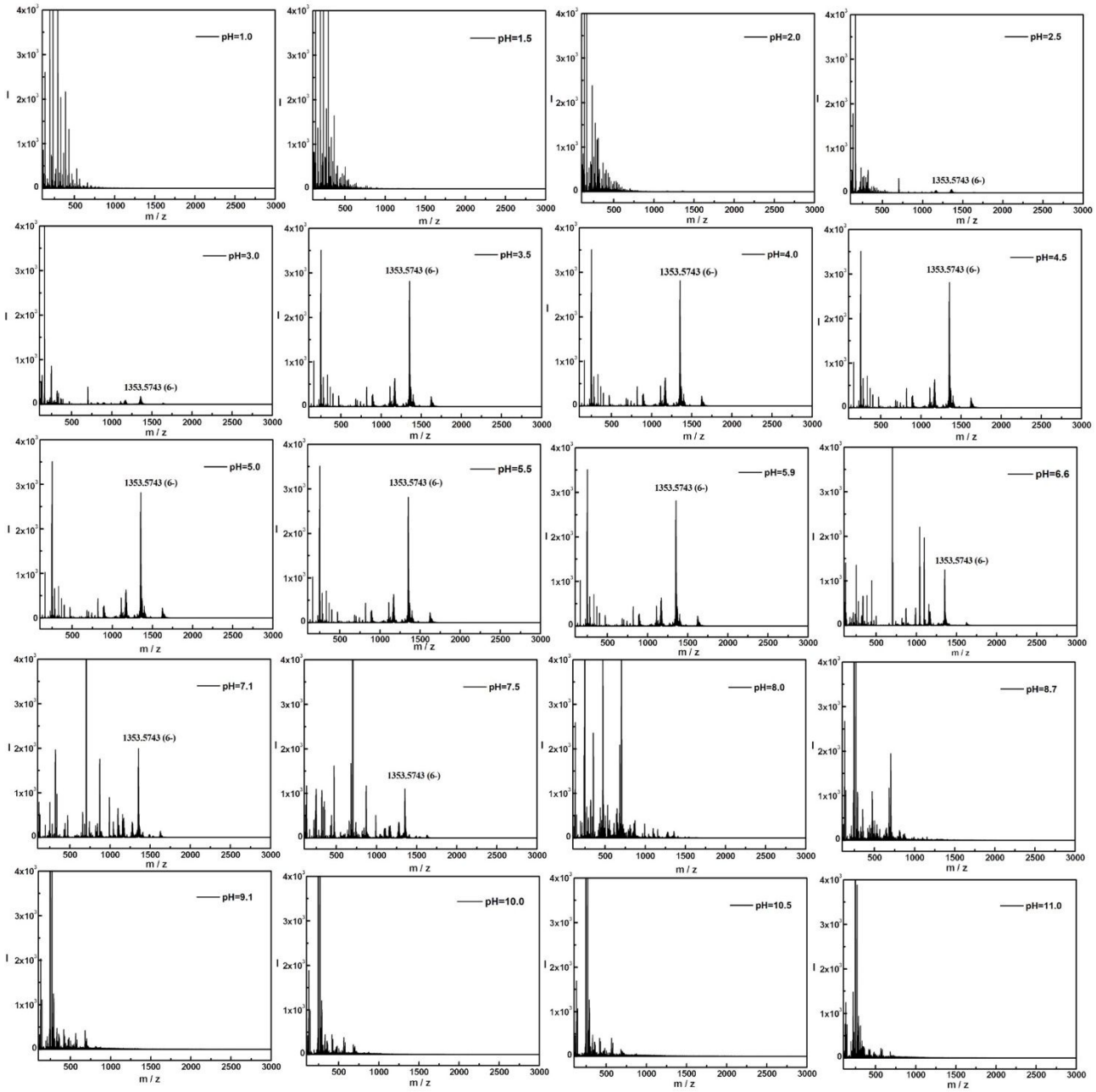

Figure S5. ESI-MS patterns of **1** at different pH values in aqueous solution.

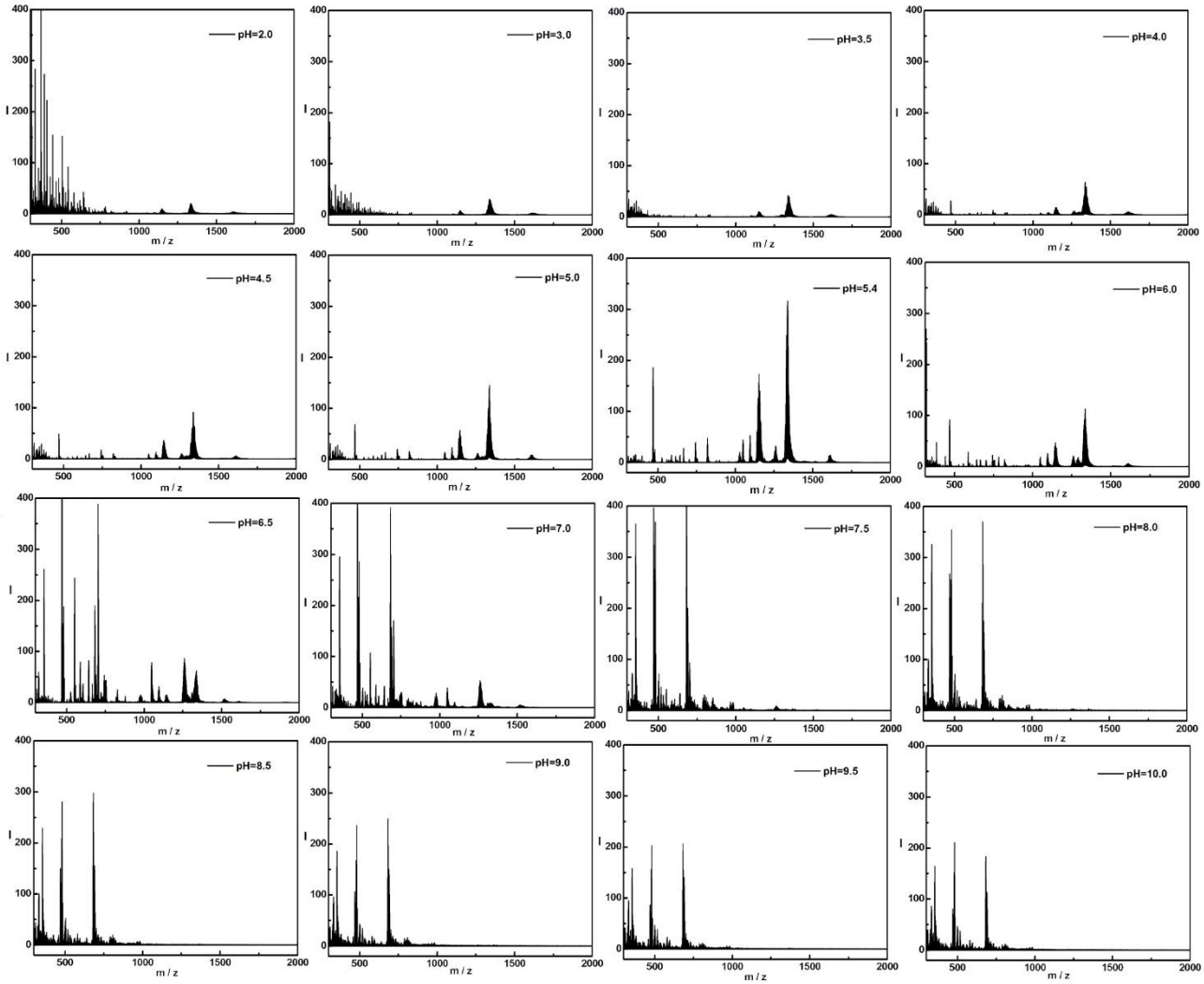

Figure S6. ESI-MS patterns of **2** at different pH values in aqueous solution.

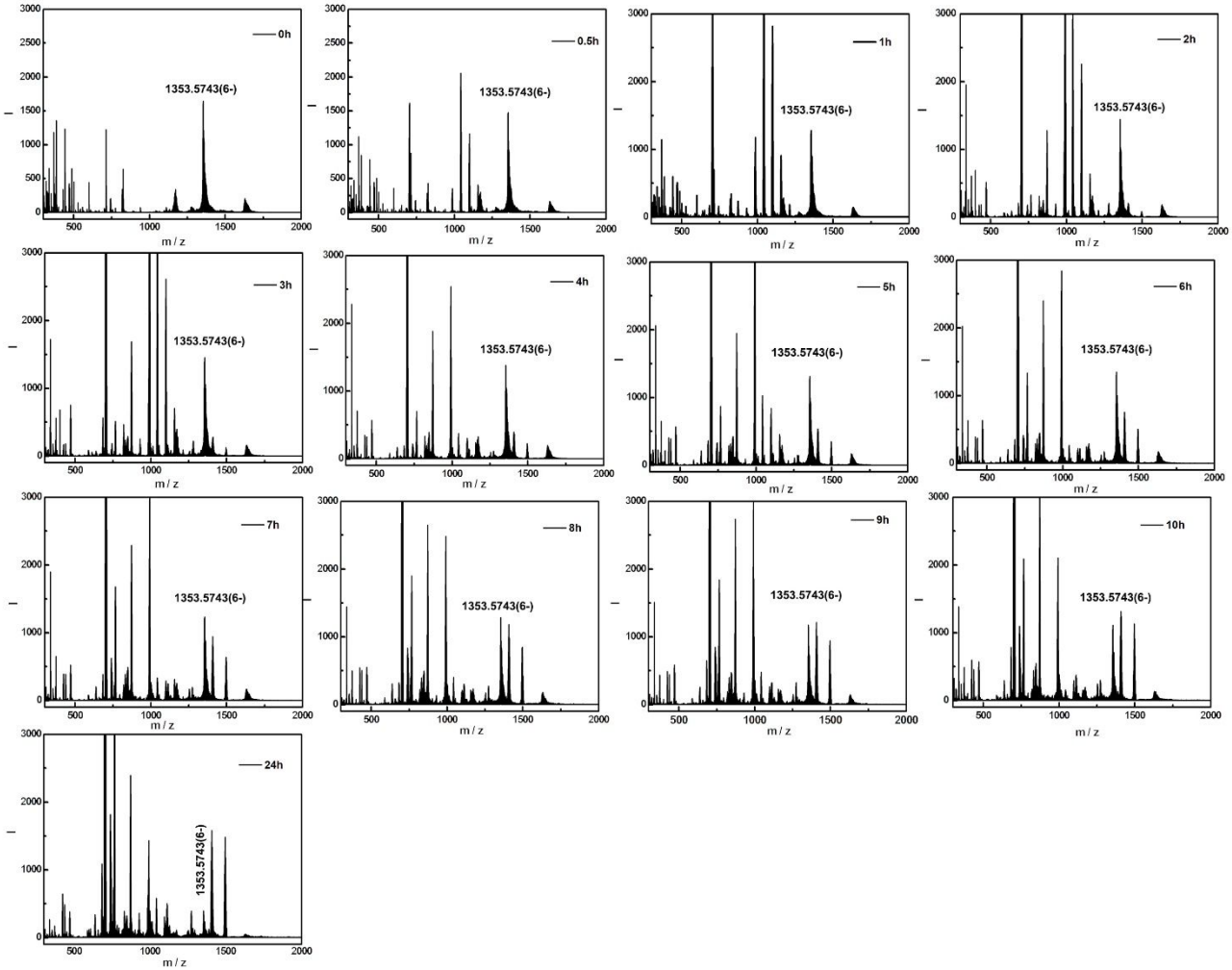

Figure S7. ESI-MS patterns of **1** at different time in aqueous solution of pH = 5.0.

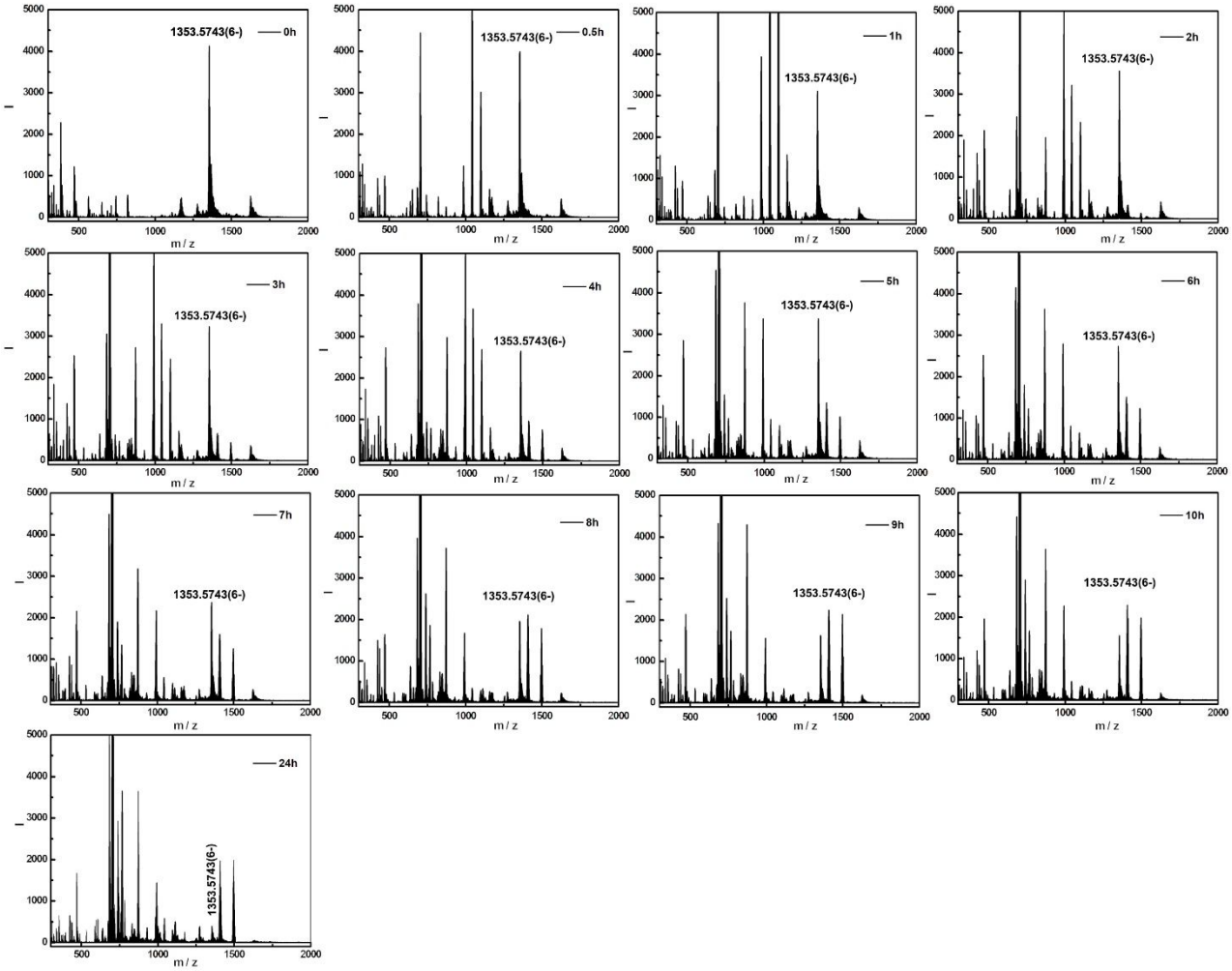

Figure S8. ESI-MS patterns of **1** at different time in aqueous solution of pH = 6.0.

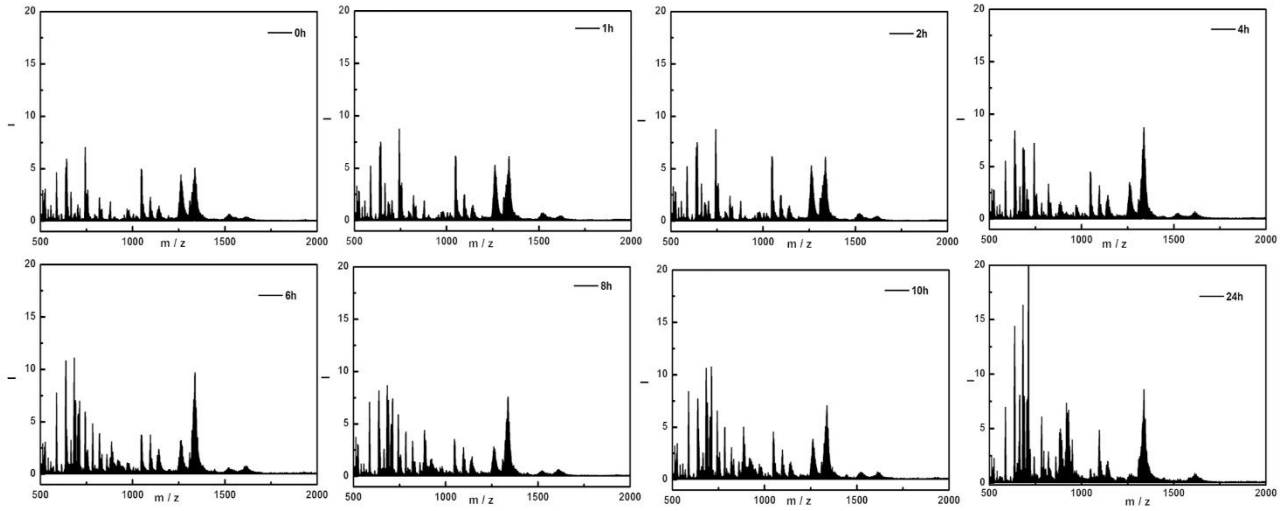

Figure S9. ESI-MS patterns of **2** at different time in aqueous solution of pH = 5.0.

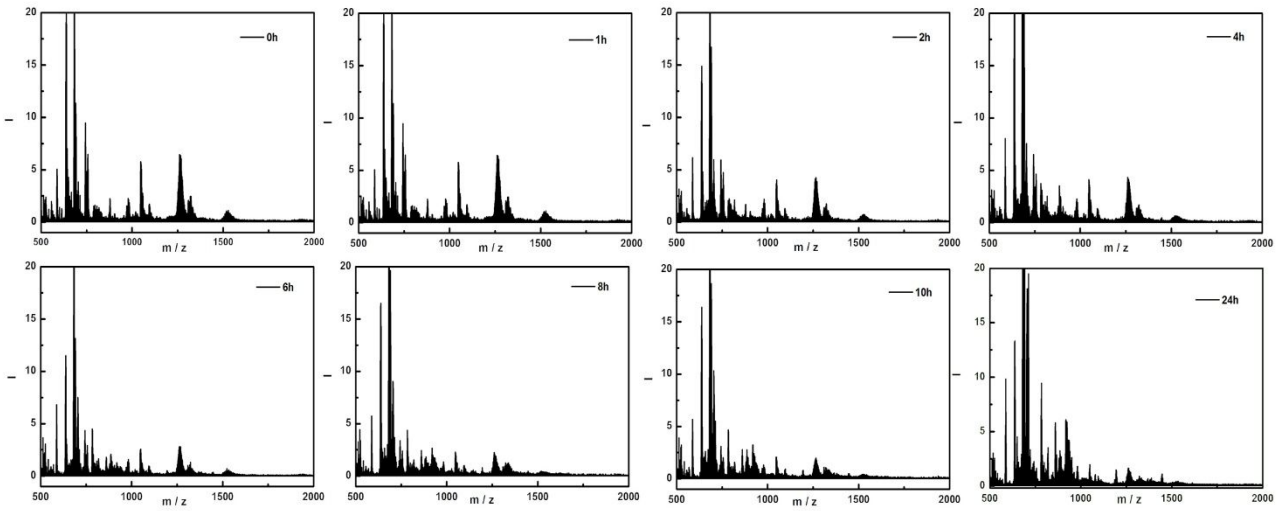

Figure S10. ESI-MS patterns of **2** at different time in aqueous solution of pH = 6.0.

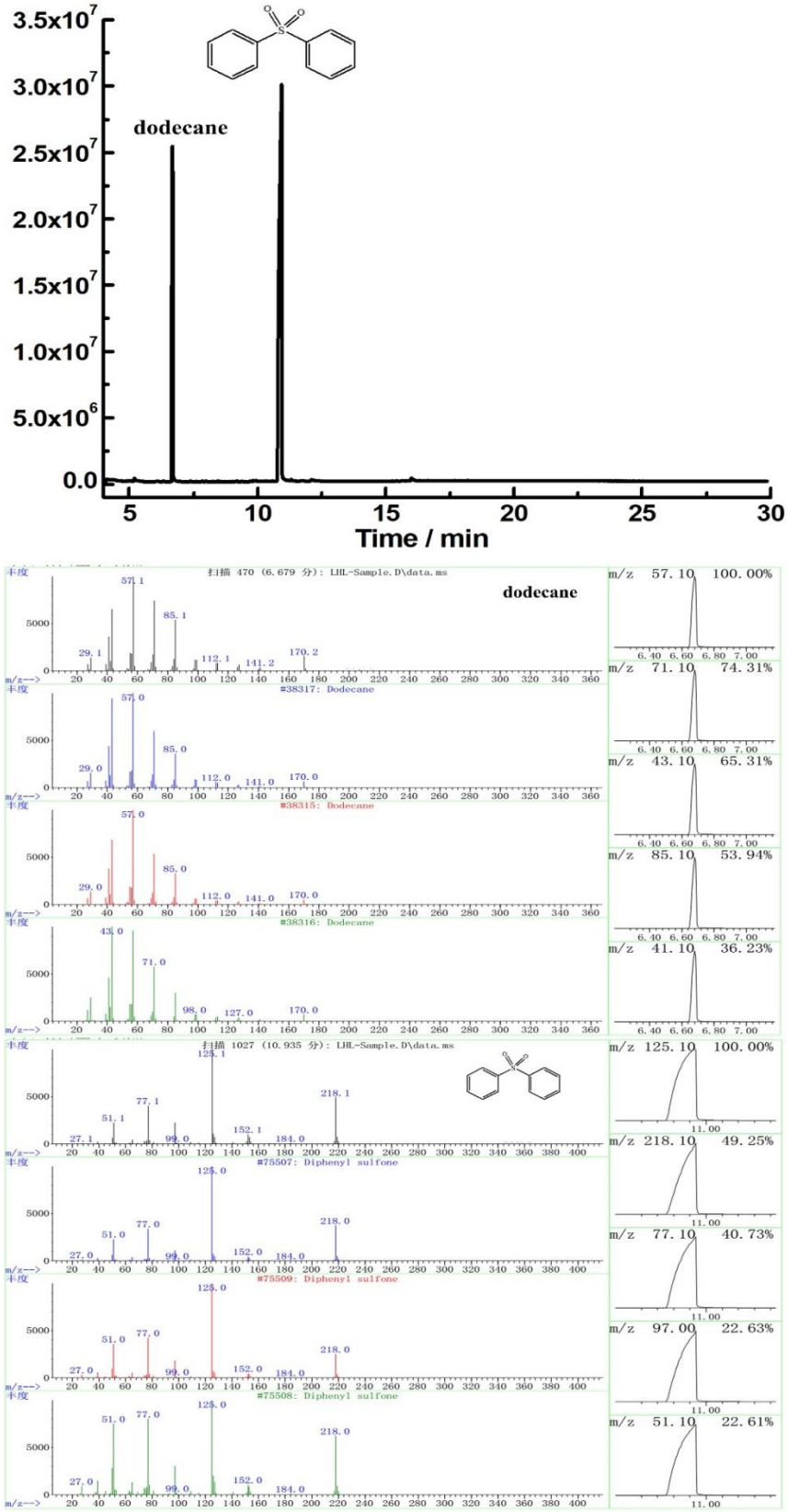

Figure S11. MS spectra for the products of DPS and dodecane and GC trace of the catalytic results for the DPSO2. Reactions conditions: DPS (0.5 mmol), 30% H_2O_2(1.5mmol) and catalyst (1.0μmol) in CH_3CN (3 mL) at 40 °C, 60 min.

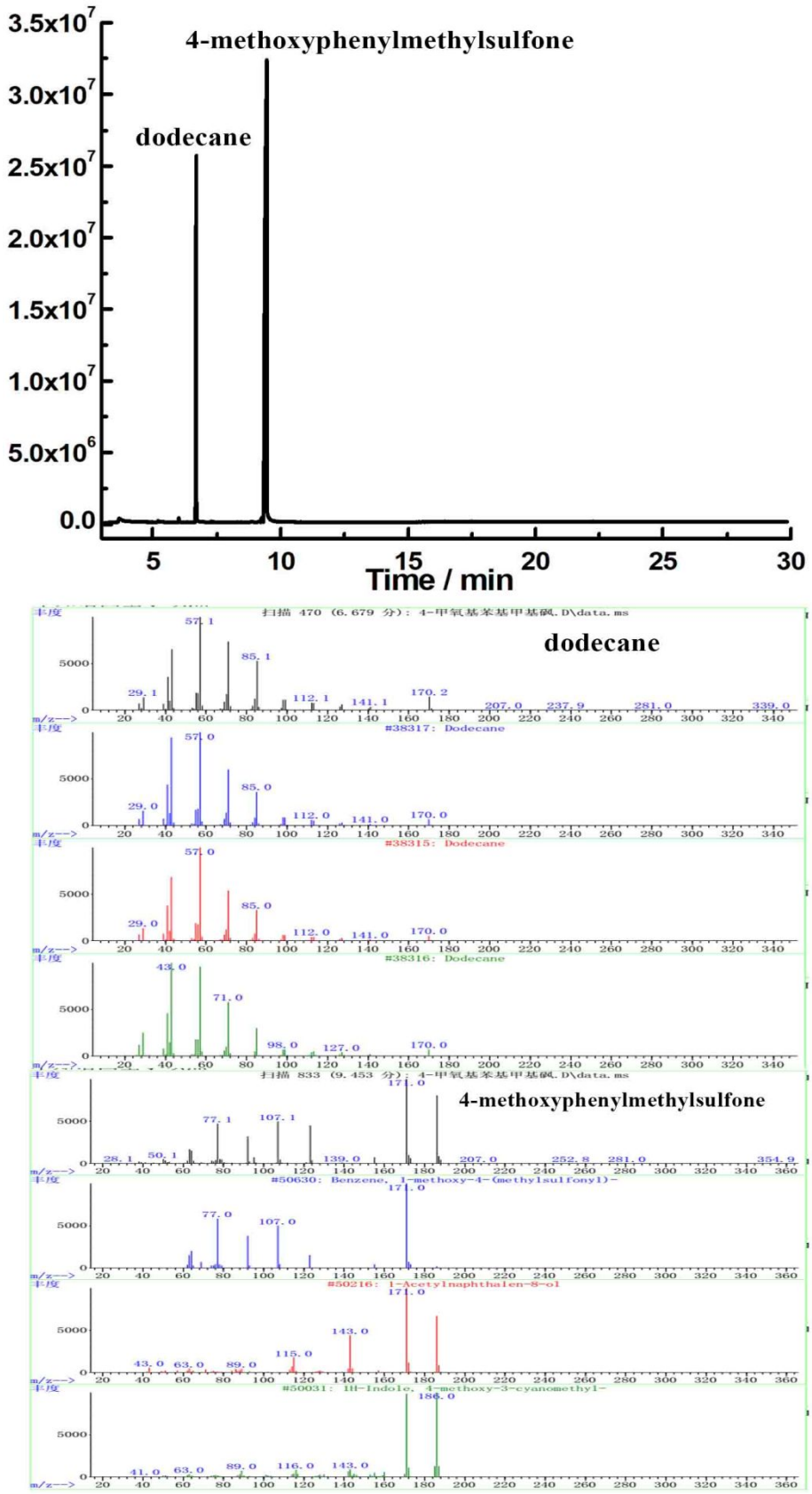

Figure S12. MS spectra for the products of 4-methoxyphenylmethylsulfide and dodecane and GC trace of the catalytic results for 4-methoxyphenylmethylsulfone. Reactions conditions: 4-methoxyphenylmethyl sulfide (0.5 mmol), 30% H_2O_2 (1.5 mmol) and catalyst (1.0 μmol) in CH_3CN (3 mL) at 40 °C, 60 min.

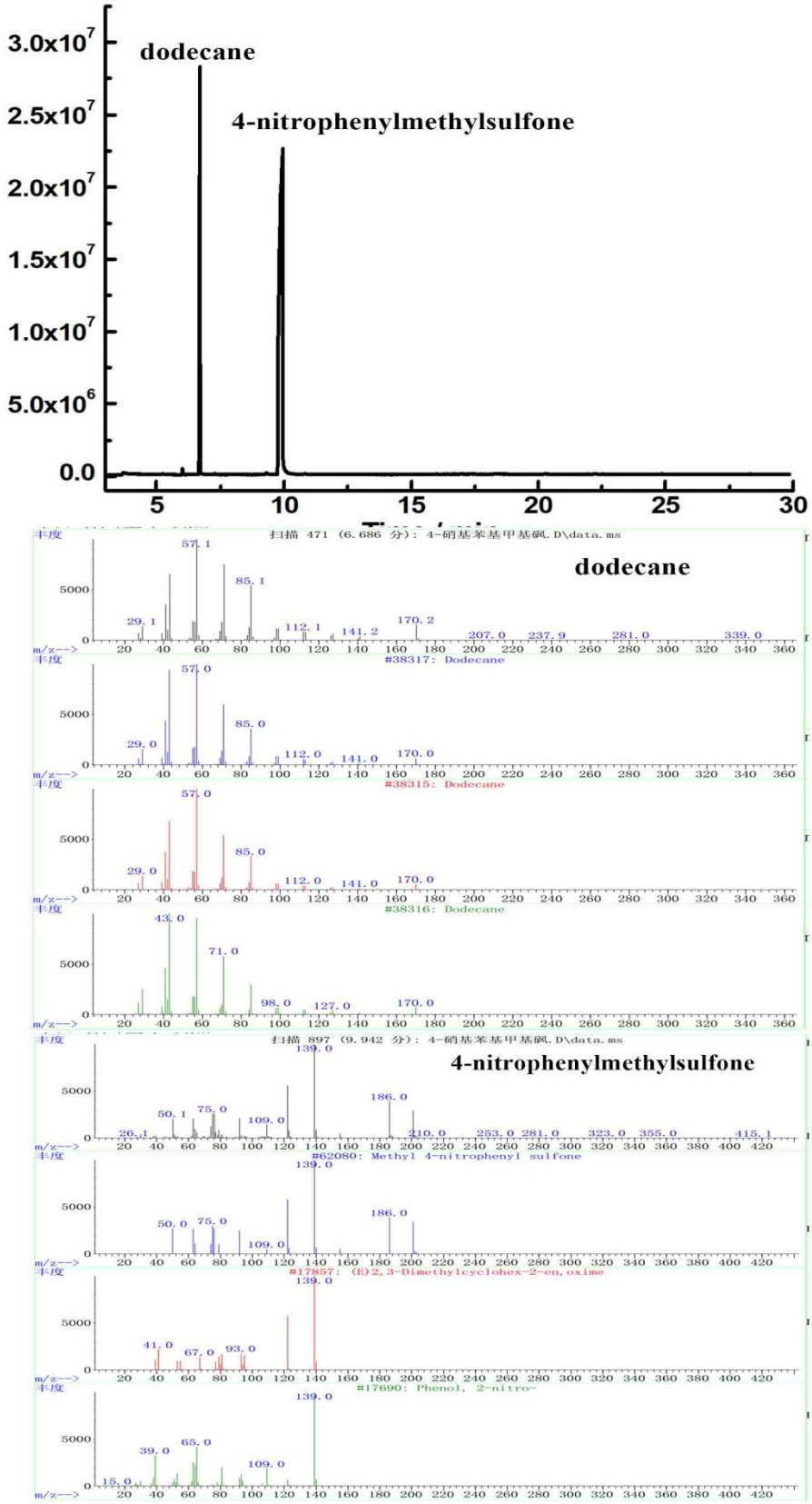

Figure S13. MS spectra for the products of 4-nitrophenylmethylsulfide and dodecane and GC trace of the catalytic results for 4-nitrophenylmethylsulfone. Reactions conditions: 4-nitrophenylmethylsulfide (0.5 mmol), 30% H_2O_2 (1.5 mmol) and catalyst (1.0 μmol) in CH_3CN (3 mL) at 40 °C, 60 min.

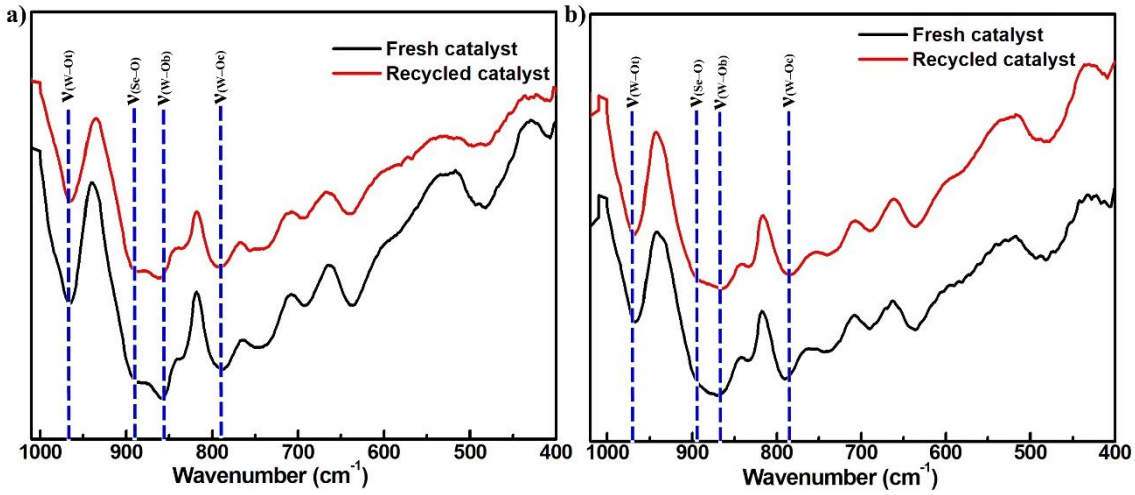

Figure S14. (a) IR spectra of fresh catalyst and recycled catalyst of **1**. (b) IR spectra of fresh catalyst and recycled catalyst of **2**.

Table S1. Crystallographic Data and Structure Refinements for 1 and 2.

	1	**2**
Empirical formula	$C_{16}H_{122}Ce_2N_6Na_4O_{142}Se_3W_{31}$	$C_{20}H_{238}Ce_4N_{10}Na_{10}O_{293}Se_6W_{62}$
Fw	8979.63	17971.04
Crystal system	Triclinic	Triclinic
Space group	P–1	*P*–1
a, Å	18.967(7)	19.710(5)
b, Å	19.027(7)	20.975 (5)
c, Å	27.182(10)	23.579 (6)
α, deg	86.512(7)	65.660(4)
β,deg	76.698(6)	77.174 (5)
γ,deg	60.394(6)	67.978(5)
V , Å^{-3}	8284(5)	8207(4)
Z	2	1
μ, mm^{-1}	22.734	22.950
F(000)	7904	7906
T, K	296(2)	296(2)
Limiting indices	-22 h ≤ 22	$-23 \le h \le 23$
	-22 *k* ≤ 22	$-15 \le k \le 24$
	-32 *l* ≤ 20	$-17 \le l \le 28$
No. of reflections collected	42693	41979
No. of independent reflections	28883	28576
R_{int}	0.0538	0.1168
Data/restrains/parameters	28883 / 34 / 1516	28576 / 332 / 1365
Goodness-of-fit on F^2	1.029	1.015
Final *R* indices [$I>2\sigma(I)$]	R_1 = 0.0556	R_1 = 0.1062

	wR_2 = 0.1252	wR_2 = 0.2208
R indices (all data)	R_1 = 0.0959	R_1 = 0.2043
	wR_2 = 0.1384	wR_2 = 0.2519

Table S2. Bond Valence Sum (BVS) Calculations of All the W, Se, Ce and O Atoms in 1.

Atom	BVS	Atom	BVS	Atom	BVS
W1	5.753	W2	5.876	W3	6.246
W4	5.899	W5	6.063	W6	6.103
W7	5.974	W8	6.162	W9	5.755
W10	5.929	W11	6.363	W12	6.169
W13	6.205	W14	5.967	W15	6.393
W16	6.154	W17	6.175	W18	5.930
W19	5.748	W20	6.093	W21	5.931
W22	5.740	W23	5.921	W24	6.047
W25	6.057	W26	5.950	W27	5.921
W28	6.264	W29	6.161	W30	6.217
W31	5.927				
Ce1	2.993	Ce2	3.013		
Se1	4.024	Se2	3.968	Se3	3.804
O1	1.937	O2	1.821	O3	1.785
O4	2.055	O5	1.759	O6	1.934
O7	1.842	O8	1.956	O9	1.926
O10	1.947	O11	1.985	O12	2.010
O13	1.793	O14	1.908	O15	1.944
O16	1.791	O17	1.871	O18	1.898
O19	1.882	O20	1.950	O21	1.982
O22	1.974	O23	2.030	O24	1.921
O25	2.054	O26	2.051	O27	1.877
O28	1.965	O29	1.960	O30	1.799
O31	1.788	O32	2.068	O33	1.935
O34	1.903	O35	1.658	O36	1.943
O37	1.896	O38	1.998	O39	2.001
O40	1.934	O41	1.913	O42	2.009
O43	2.173	O44	1.952	O45	1.821
O46	2.006	O47	1.953	O48	1.867
O49	1.882	O50	1.860	O51	1.842
O52	1.822	O53	0.407	O54	1.875

O55	2.011	O56	1.885	O57	1.792
O58	1.920	O59	1.712	O60	1.635
O61	1.807	O62	1.789	O63	1.994
O64	1.932	O65	1.662	O66	1.973
O67	2.075	O68	0.983	O69	1.570
O70	1.978	O71	1.988	O72	1.740
O73	1.970	O74	1.919	O75	1.842
O76	1.275	O77	1.862	O78	1.946
O79	1.662	O80	1.887	O81	1.826
O82	1.973	O83	1.958	O84	1.774
O85	1.671	O86	2.005	O87	0.315
O88	2.000	O89	1.782	O90	2.080
O91	1.989	O92	1.852	O93	2.030
O94	1.613	O95	2.006	O96	1.736
O97	1.778	O98	1.649	O99	1.905
O100	1.694	O101	2.003	O102	1.712
O103	1.812	O104	2.004	O105	1.849
O106	1.600	O107	1.506	O108	1.911
O109	1.882	O110	1.694	O111	1.759

Table S3. Bond Valence Sum (BVS) Calculations of All the W, Se, Ce and O Atoms in 2.

Atom	BVS	Atom	BVS	Atom	BVS
W1	5.733	W2	6.247	W3	6.290
W4	6.438	W5	6.832	W6	6.649
W7	6.665	W8	6.184	W9	6.275
W10	6.637	W11	6.160	W12	6.659
W13	6.464	W14	6.114	W15	5.877
W16	6.420	W17	6.141	W18	6.474
W19	6.391	W20	6.572	W21	6.206
W22	6.753	W23	5.966	W24	6.579
W25	5.992	W26	5.992	W27	6.606
W28	6.461	W29	6.513	W30	6.343
W31	6.189				
Ce1	3.175	Ce2	2.849		
Se1	4.121	Se2	3.931	Se3	4.093
O1	2.254	O2	2.007	O3	1.835
O4	2.015	O5	1.823	O6	1.976

O7	2.044	O8	2.019	O9	1.967
O10	1.979	O11	1.915	O12	2.115
O13	2.308	O14	1.960	O15	2.136
O16	2.020	O17	1.924	O18	1.897
O19	2.131	O20	2.081	O21	1.977
O22	1.977	O23	2.028	O24	2.003
O25	2.080	O26	2.133	O27	2.277
O28	1.992	O29	2.023	O30	2.079
O31	2.018	O32	2.075	O33	1.990
O34	2.016	O35	2.082	O36	2.066
O37	2.028	O38	2.138	O39	2.116
O40	2.071	O41	2.000	O42	2.017
O43	2.082	O44	1.926	O45	2.015
O46	1.976	O47	2.068	O48	1.707
O49	2.015	O50	1.998	O51	2.073
O52	1.662	O53	2.026	O54	1.961
O55	2.075	O56	0.450	O57	2.232
O58	2.087	O59	2.213	O60	0.351
O61	2.152	O62	2.004	O63	2.102
O64	2.058	O65	1.831	O66	1.707
O67	2.084	O68	2.142	O69	1.671
O70	2.075	O71	1.528	O72	2.201
O73	1.960	O74	2.083	O75	1.850
O76	1.958	O77	1.676	O78	2.037
O79	1.792	O80	2.030	O81	1.797
O82	2.052	O83	1.912	O84	1.657
O85	1.812	O86	1.958	O87	1.944
O88	1.657	O89	2.020	O90	1.832
O91	1.960	O92	2.052	O93	2.033
O94	1.689	O95	1.635	O96	2.007
O97	1.837	O98	1.703	O99	2.022
O100	1.975	O101	1.675	O102	1.549
O103	1.764	O104	1.847	O105	1.960
O106	1.703	O107	2.002	O108	2.091
O109	2.038	O110	1.817		